Chapter 4

Modelling of Temporal-Spatial Distribution of Airplane Wake Vortex for Scattering Analysis

Jianbing Li, Zhongxun Liu and Xuesong Wang

Additional information is available at the end of the chapter

http://dx.doi.org/10.5772/66544

Abstract

Aircraft wake vortex is a pair of intensive counter-rotating airflow generated by a flying aircraft. Wake vortex is one of the most dangerous hazards in aviation because it may cause a following aircraft to roll out of control, particularly during the taking off and landing phases. The real-time detection of wake vortex is a frontier scientific problem emerging from many fields like aviation safety and atmospheric physics, and the dynamics and scattering characteristics of it remain as key problems to develop corresponding detection technologies. This chapter aims at presenting a simulation scheme for the dynamics of wake vortex under different weather conditions. For wake vortex generated in clear air, changes of the atmospheric dielectric constant produced by the density variation and water vapour variation are analysed; for wake vortex generated in rainy condition, the raindrop distribution in the wake vortex is also analysed. Both of them are essential for further analysing the scattering characteristics and developing new detection algorithms.

Keywords: wake vortex, dynamics, clear air, wet weather

1. Introduction

Wake vortex is an inevitable physical phenomenon that exists in the rear zone of a flying aircraft, which rotates intensively and has a complex structure. The wake vortex generated by a large aircraft could be very hazardous to aviation safety since it might cause a following aircraft to roll out of control, particularly during the departure and landing phases.

In Air Traffic Management (ATM) field, International Civil Aviation Organization (ICAO) established a series of flight interval rules. These rules can ensure the flight safety in most time, but they are too conservative. In order to reach a good balance between avoiding the encountering

hazard of wake vortex and increasing the transport capacity of airports, much attention has been paid on the real-time monitoring and detection of wake vortex in the past decades. Some major ATM programmes like Single European Sky ATM Research (SESAR) and Next Generation Air Transportation System, USA (NextGen) have also launched many projects on this topic, and the representative research institutes include Thales, Office National d'Etudes et de Recherches Aerospatiales (ONERA), Deutsches Zentrum für Luft- und Raumfahrt e.V. (DLR), Université catholique de Louvain (UCL), National Aeronautics and Space Administration (NASA), Federal Aviation Administration (FAA), Lincoln Lab, Boeing, and so on. In all these studies, the characteristics, detection technology and parameter retrieval are the key issues, and the characteristics of wake vortex serve as the basis for the rest studies.

In aviation safety, we mainly concern the clear air condition and wet weather condition. According to the scattering theory, the scattering of wake vortex in clear air is mainly determined by the fluctuation of dielectric constant inside the wake; while under wet condition, the key scattering factor becomes the massive number of precipitation droplets carried by the velocity of wake vortex. In this chapter, we present simulation schemes for the dielectric constant distribution and droplet distribution of wake vortex. The distributions are caused by the dynamics of wake vortex and serve as the physical basis for scattering analysis.

First, we study the dielectric constant distribution of wake vortex generated in clear air.

2. Dielectric constant of wake vortex generated in clear air

2.1. Two key parameters for determining the dielectric constant of wake vortex

The relative dielectric constant of atmosphere (ε_{r}) can be well depicted by the following expression [1]:

$$\varepsilon_{\mathrm{r}} = \left[1 + 0.776 \times 10^{-6} \frac{p}{T}\left(1 + \frac{7780q}{T}\right)\right]^2 \tag{1}$$

where p,T,q are the pressure (pa), absolute temperature (K), and water vapour content (kg/kg), respectively. Generally, the second term in the square bracket is much smaller than 1, so the variation in dielectric constant between wake vortex and ambient air can be approximated as follows when the Taylor expansion is taken into account:

$$\Delta\varepsilon_{\mathrm{r}} = \varepsilon_{\mathrm{r}} - \varepsilon_{\mathrm{r,a}} \approx 1.552 \times 10^{-6}\left[\frac{p}{T}\left(1 + \frac{7780q}{T}\right) - \frac{p_{\mathrm{a}}}{T_{\mathrm{a}}}\left(1 + \frac{7780q_{\mathrm{a}}}{T_{\mathrm{a}}}\right)\right] \tag{2}$$

In the expression, the parameters with subscript “a” refer to the ambient parameters and those without “a” refer to the wake vortex's parameters.

As is known, an isentropic process is a process in which there is neither heat exchange nor any friction effect [2]. Typically, the wake vortex of a subsonic airplane can be assumed as an isentropic flow, and the thermodynamic parameters at different points along a streamline can be written as follows:

$$\frac{p}{p_a} = \left(\frac{\rho}{\rho_a}\right)^{\gamma}, \frac{T}{T_a} = \left(\frac{\rho}{\rho_a}\right)^{\gamma-1} \tag{3}$$

where $\gamma = 1.4$ is the adiabatic coefficient for air. Consequently, the variation in dielectric constant is transformed to

$$\Delta\varepsilon_r \approx 1.552\times10^{-6}\times\left[\frac{p_a}{T_a}(\xi-1) + 7780\frac{p_a}{{T_a}^2}(\xi^{2-\gamma}q - q_a)\right] \tag{4}$$

Here we have denoted $\xi = \rho/\rho_a$, and the effects due to density and water vapour are mixed in the term $\xi^{2-\gamma}q$. In order to separate the two factors, this term is transformed to

$$\xi^{2-\gamma}q = [1 + (\xi-1)]^{2-\gamma}(q_a + \Delta q) \tag{5}$$

with $\Delta q = q - q_a$ being the water vapour variation between the local wake and the ambient air. Since the variations in density and water vapour for wake vortex are very small, say $\xi - 1 << 1$ and $\Delta q << q_a$, the dielectric constant variation can be approximated as follows when the Taylor expansion is adopted:

$$\Delta\varepsilon_r \approx 1.552\times10^{-6}\frac{p_a}{{T_a}^2}\times\{[T_a + 7780(2-\gamma)q_a](\xi-1) + 7780\Delta q\} \tag{6}$$

In this expression there are two undetermined parameters, ξ and Δq. They are separated into two different terms:

$$\Delta\varepsilon_r = \Delta\varepsilon_r^d + \Delta\varepsilon_r^v \tag{7}$$

The first term is determined by the density variation ξ:

$$\Delta\varepsilon_r^d \approx 1.552\times10^{-6}\frac{p_a}{{T_a}^2}(T_a + 4668q_a)(\xi-1) \tag{8}$$

and the second term is determined by the water vapour variation Δq:

$$\Delta\varepsilon_r^v \approx 1.207\times10^{-2}\frac{p_a}{{T_a}^2}\Delta q \tag{9}$$

In this manner, the key of modelling the dielectric constant is to determine the two parameters, ξ and Δq.

2.2. Effect of density variation on the dielectric constant

2.2.1. Velocity field of wake vortex

When the stationary phase of a subsonic wake vortex is taken into account, the dynamics can be well characterized by the steady Lamb momentum equation [2]:

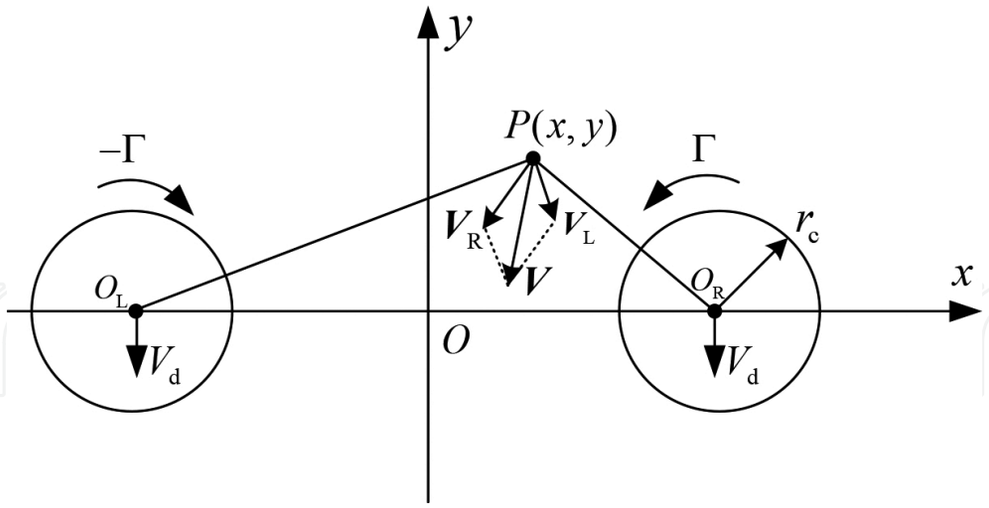

Figure 1. Velocity of counter-rotating vortices.

$$\boldsymbol{\Omega}\times\boldsymbol{V}+\frac{1}{2}|\boldsymbol{V}|^2=-\frac{1}{\rho}\nabla p \tag{10}$$

where **V** is the total velocity of wake vortex, and $\Omega = \nabla\times\mathbf{V}$ is the vorticity. In this expression, the velocity and density are separated, which makes it convenient to work out the thermodynamics parameters according to the velocity field.

Typically, when no cross-wind is considered, a stable-stage wake is composed of two contour rotating vortices of the same strength, and they descend at a velocity V_d. In this manner, in a coordinate system descending with the vortex cores, the wake vortex is steady, and the velocity for a given point P can be written as (see **Figure 1**):

$$\boldsymbol{V}=-\boldsymbol{V}_\mathrm{d}+\boldsymbol{V}_\mathrm{L}+\boldsymbol{V}_\mathrm{R} \tag{11}$$

where $\boldsymbol{V}_\mathrm{L}$ and $\boldsymbol{V}_\mathrm{R}$ are the velocities deduced by the left and right vortices, and $\mathbf{V}_\mathrm{d}$ is the descending velocity. In **Figure 1**, the parameter Γ is the circulation which defines the strength of the wake vortex.

- In the expression, the deduced velocity of each vortex can be presented by existing velocity profile models, such as Rankine model, Lamb-Oseen model, and so on. Among them, the Rankine model is a widely used one, and the corresponding tangential velocity (V_θ) follows [3]:

$$V_\theta(r)=\frac{\Gamma_0}{2\pi r}\begin{cases} r^2/r_\mathrm{c}^2, & r<r_\mathrm{c} \\ 1, & r\geq r_\mathrm{c}\end{cases} \tag{12}$$

where r is the distance of a given point to the vortex centre, $r_c \approx 0.052 b_0$ the vortex core radius, and b_0 the vortex spacing. As shown in **Figure 2**, the velocity outside the vortex core is irrotational, while the inside part is with a uniform vorticity:

http://dx.doi.org/10.5772/66544

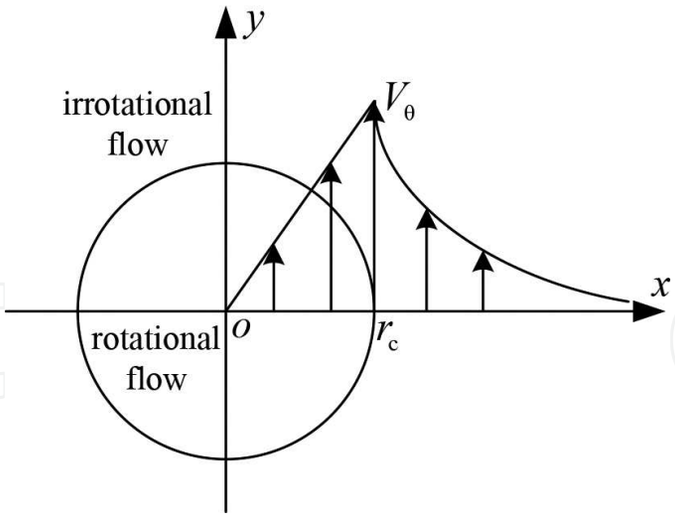

Figure 2. Rankine velocity profile.

$$\omega_0 = \frac{\Gamma_0}{\pi r_c^2} \tag{13}$$

- The descending velocity can be derived from the deduced velocity of a vortex core:

$$\boldsymbol{V}_d = -\frac{\Gamma_0}{2\pi b_0}\hat{y} \tag{14}$$

2.2.2. Stream function of wake vortex

When the velocity components are determined, the vorticity is finally obtained as

$$\boldsymbol{\Omega} = \nabla \times \boldsymbol{V} = \omega_0 H(\boldsymbol{r}) \tag{15}$$

In this expression, we have considered $\nabla \times \boldsymbol{V}_d = 0$, and $H(\mathbf{r})$ is an identification function for the left vortex core region (C_L) and right one (C_R):

$$H(\boldsymbol{r}) = \begin{cases} -1, & \boldsymbol{r} \in C_L \\ 1, & \boldsymbol{r} \in C_R \\ 0, & \text{otherwise} \end{cases} \tag{16}$$

As a result, we have

$$\boldsymbol{\Omega} \times \boldsymbol{V} = \omega_0 H(\boldsymbol{r})(-v\hat{x} + u\hat{y}) = \omega_0 H(\boldsymbol{r})\nabla\psi \tag{17}$$

where u and v are the velocity components in x and y directions, and ψ is the stream function:

$$u = \frac{\partial\psi}{\partial y}, v = -\frac{\partial\psi}{\partial x} \tag{18}$$

In this manner, the Lamb momentum equation for wake vortex is rewritten as

$$\omega_0 H(\boldsymbol{r})\nabla\psi + \frac{1}{2}|\boldsymbol{V}|^2 = -\frac{1}{\rho}\nabla p. \tag{19}$$

Furthermore, integrating the above equation from a point $\boldsymbol{r}$ to infinity gives

$$I = -\omega_0 H(\boldsymbol{r})\psi + \frac{1}{2}V_{\mathrm{d}}^2 - \frac{1}{2}|\boldsymbol{V}|^2 = -\int_r^\infty \frac{1}{\rho}\mathrm{d}p \tag{20}$$

where we have considered $\mathbf{V}_\infty = V_{\mathrm{d}}\hat{y}$, and the total stream function ψ is

$$\psi = -V_{\mathrm{d}}x + \psi_{\mathrm{L}} + \psi_{\mathrm{R}} + C \tag{21}$$

with the four terms on the right-hand side being the up-wash flow at infinity, the stream function due to the left vortex and right vortex, and a constant.

For a Rankine vortex, the stream function follows

$$\psi_{\mathrm{Rankine}} = -\frac{\Gamma}{4\pi}\begin{cases} \dfrac{r^2}{r_0^2} - 1 + \ln r_0^2, & r < r_{\mathrm{c}}; \\ \ln r^2, & r \geq r_{\mathrm{c}}. \end{cases} \tag{22}$$

Then ψ_{L} and ψ_{R} can be obtained by replacing the circulation Γ with $-\Gamma_0$ and Γ_0, respectively.

Also, the constant C is chosen to meet $\psi(\boldsymbol{r}) = 0$ when $\boldsymbol{r}$ is on the vortex core boundary:

$$C = \psi_1(\boldsymbol{r}) = V_{\mathrm{d}}x - \psi_{\mathrm{L}} - \psi_{\mathrm{R}} \tag{23}$$

Due to the impact between two vortices, the constant C has a very slight variation along the vortex core boundary. In practice, the average of $\psi_1(\boldsymbol{r})$ along one vortex core boundary is chosen as the constant.

As a result, combination of the total stream function and velocity gives the distribution of integral I as shown in Eq. (20), which is then used to calculate the density distribution of wake vortex.

2.2.3. Determination of dielectric constant due to density variation

Substituting the isentropic relationship (3) into the item on the right hand of Eq. (20) gives

$$I = -\int_{\mathrm{r}}^\infty \frac{1}{\rho}\mathrm{d}p = -\int_{\mathrm{r}}^\infty \frac{\gamma}{\gamma-1}\frac{p_{\mathrm{a}}}{\rho_{\mathrm{a}}^\gamma}\mathrm{d}\rho^{\gamma-1} = \frac{\gamma}{\gamma-1}\frac{p_{\mathrm{a}}}{\rho_{\mathrm{a}}^\gamma}(\rho^{\gamma-1} - \rho_{\mathrm{a}}^{\gamma-1}) \tag{24}$$

which can then be transformed as

$$\xi = \frac{\rho}{\rho_{\mathrm{a}}} = \left[1 + \frac{(\gamma-1)\rho_{\mathrm{a}}}{\gamma p_{\mathrm{a}}}I\right]^{\frac{1}{\gamma-1}} \tag{25}$$

For a wake vortex, the integral I has the same magnitude as V_θ^2 (generally not larger than 1000). On the other hand, ρ_a and p_a are, respectively, on the magnitude of 1 and 10^5. Therefore, the second term in Eq. (25) is much smaller than 1, and the Taylor expansion gives:

$$\xi \approx 1 + \frac{\rho_a}{\gamma p_a} I \tag{26}$$

Consequently, the effects of dielectric constant can be rewritten as

$$\Delta \varepsilon_r^d(\boldsymbol{r}) \approx 1.552 \times 10^{-6} \frac{p_a (T_a + 4668 q_a)}{\gamma R T_a^3} I(\boldsymbol{r}). \tag{27}$$

2.3. Effect of water vapour variation on the dielectric constant

Generally, the atmospheric water vapour inside the wake vortex can be modelled as a passive scalar, which is convected by the wake vortex velocity field and is governed by the convection-diffusion equation [4]:

$$\frac{\partial q}{\partial t} + (\boldsymbol{V} \cdot \nabla) q - D \nabla^2 q = 0, \tag{28}$$

where q is the water vapour concentration, D is the diffusion coefficient for an air/water vapour system, and $\mathbf{V}$ is the velocity filed of a wake.

In fluid dynamics, the Péclet number is a dimensionless number indicating the rates of convection and diffusion of a flow [5]:

$$\mathrm{P_e} = \frac{UL}{D} \tag{29}$$

where L is the characteristic length, U is the velocity, and D is the mass diffusion coefficient. Generally, a flow is convection-dominated, if the Péclet number is large. In this study, the diffusion coefficient for air ($D = 2.42 \times 10^{-5}$) is very small, which leads to a big Péclet number and the flow is convection dominated. In this manner, neglecting the impact of diffusion leads to a simplified governing equation:

$$\frac{\partial q}{\partial t} + (\boldsymbol{V} \cdot \nabla) q = 0 \tag{30}$$

As is known, the initial water vapour gradient is very important to characterize the equation. Here the stratified model is adopted in this work

$$q(\boldsymbol{r}, t)|_{t=0} = q_a = m_q (y - y_0) + q_0 \tag{31}$$

with q_0 and m_q being the offset and gradient of water vapour content, respectively. Substituting the initial condition into the governing equation gives

$$\frac{\partial q(\boldsymbol{r},0)}{\partial t}+(\boldsymbol{V}\cdot\nabla)q(\boldsymbol{r},0)=V_y m_q \tag{32}$$

Therefore, Eq. (30) minus Eq. (32) leads to a new equation:

$$\frac{\partial Q}{\partial t}+(\boldsymbol{V}\cdot\nabla)Q=-V_y m_q \tag{33}$$

with $Q(\boldsymbol{r},t)=\Delta q(\boldsymbol{r},t)=q(\boldsymbol{r},t)-q(\boldsymbol{r},0)$ being the water vapour variation. At the same time, the initial condition of Eq. (33) becomes $Q(\boldsymbol{r},t)|_{t=0}=q(\boldsymbol{r},t)|_{t=0}-q(\boldsymbol{r},0)=0$; this is coincident with the physical image that the water vapour variation is initially zero.

Eq. (33) is a hyperbola differential equation, which is often numerically difficult to solve. In the present work, the leapfrog scheme is adopted to solve the target equation, and good convergence and stability are achieved. The scheme is as follows:

$$\frac{Q_{i,j}^{n+1}-Q_{i,j}^{n-1}}{2\Delta t}+u\frac{Q_{i+1,j}^{n}-Q_{i-1,j}^{n}}{2\Delta x}+v\frac{Q_{i,j+1}^{n}-Q_{i,j-1}^{n}}{2\Delta x}=-v_{i,j}m_q, \tag{34}$$

with u and v being the velocity components in x and y direction, respectively. In the process, the Von Neumann method leads to the following stable condition [6]:

$$\Delta t<\frac{1}{2}\frac{\Delta}{V_{\max}} \tag{35}$$

where Δt is the time step, Δ is the minimum grid spacing, and $V_{\max}$ is the maximum velocity in the wake vortex.

In addition, non-uniform grids and symmetric condition are used to reduce computational cost. On the one hand, the velocity distribution shows that the flow in and around the vortex core is relatively complex and the flow far from the vortex core is slowly variational. Typically, sparse grids are adequate to characterize the slowly variational zones, but complex zones require dense grids. In this manner, non-uniform grid scheme can be adopted to reduce the total number of grids. On the other hand, the wake vortex is symmetric, so only half of wake vortex needs to be computed. Overall much computational cost can be saved through the above scheme.

If the water vapour variation, $Q(\boldsymbol{r},t)$ is solved from Eq. (33), then $\Delta\varepsilon_r^v$ can be immediately obtained according to Eq. (9).

In this above simulation, the moving coordinate system is also used. The dielectric constant distribution can be transformed into the stationary coordinate system if the following transform is used:

http://dx.doi.org/10.5772/66544

$$y' = y - V_{\mathrm{d}} \cdot t \tag{36}$$

where V_{d} is the descending velocity, t is the evolutional time, y and y' are the coordinates in the moving coordinate system and stationary coordinate system, respectively.

2.4. Numerical examples

Here we give several numerical examples for the dielectric constant distribution due to different effects. The parameters of airplane and atmosphere are as shown in **Table 1**.

According to the parameters, the distribution of $I(\boldsymbol{r})$ can be worked out, and the intensity of dielectric constant due to density variation can be obtained as shown in **Figure 3**. It is observed that $\Delta\varepsilon_{\mathrm{r}}^{\mathrm{d}}$ in the vortex cores are much larger than that outside, so the vortex core could present a big contribution to the scattering of wake vortex.

The dielectric constant due to water vapour variation ($\Delta\varepsilon_{\mathrm{r}}^{\mathrm{v}}$) can be obtained when the given partial equation (33) is solved, and **Figure 4** presents $\Delta\varepsilon_{\mathrm{r}}^{\mathrm{v}}$ at $t = 40$s. It is observed that the convection effect of water vapour results in a non-uniform laminar structure in and around the wake vortex cores, and these structures could be good contributor to the scattering in high frequency.

Consequently, the sum of **Figures 3** and **4** gives the total distribution of dielectric constant (see **Figure 5**). Comparing the magnitude of $\Delta\varepsilon_{\mathrm{r}}^{\mathrm{d}}$ and that of $\Delta\varepsilon_{\mathrm{r}}^{\mathrm{v}}$ shows that $\Delta\varepsilon_{\mathrm{r}}^{\mathrm{v}}$ is much less than $\Delta\varepsilon_{\mathrm{r}}^{\mathrm{d}}$, and $\Delta\varepsilon_{\mathrm{r}}^{\mathrm{d}}$ dominates the magnitude of $\Delta\varepsilon_{\mathrm{r}}$. However, $\Delta\varepsilon_{\mathrm{r}}^{\mathrm{d}}$ and $\Delta\varepsilon_{\mathrm{r}}^{\mathrm{v}}$ have different structures; they make different contribution to the scattering in different frequency bands. Typically, the scattering of clear air wake vortex at a frequency lower than 100MHz is mainly determined by the density variation $\Delta\varepsilon_{\mathrm{r}}^{\mathrm{d}}$; otherwise, the water vapour variation $\Delta\varepsilon_{\mathrm{r}}^{\mathrm{v}}$ makes the major contribution.

2.5. Extrapolation of dielectric constant distribution

The extrapolation includes two parts: one is relate to the density distribution and another is related to the water vapour distribution.

Parameters	Value
Airplane mass M	250,000 kg
Wingspan B	68 m
Speed V	133 m/s
Ambient pressure p_a	100,000 pa
Ambient absolute temperature T_a	288 K
Diffusion constant D	$2.42\times10^{-5}\mathrm{m}^2/\mathrm{s}$
Water vapour content offset q_0	0.018 kg/kg
Water vapour content gradient m_q	-8×10^{-8} kg/(m kg)

Table 1. Parameters of airplane and atmosphere.

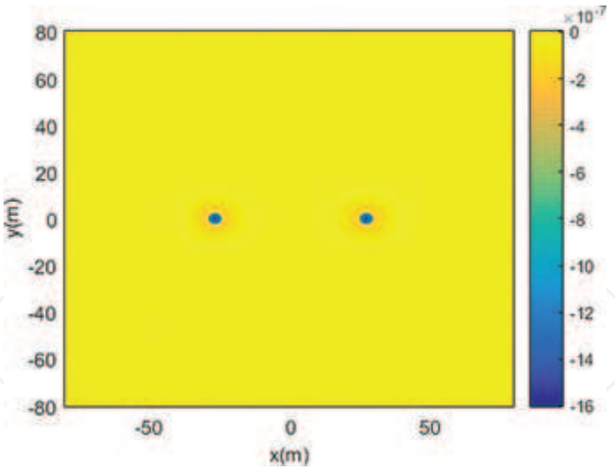

Figure 3. Dielectric constant distribution due to density variation.

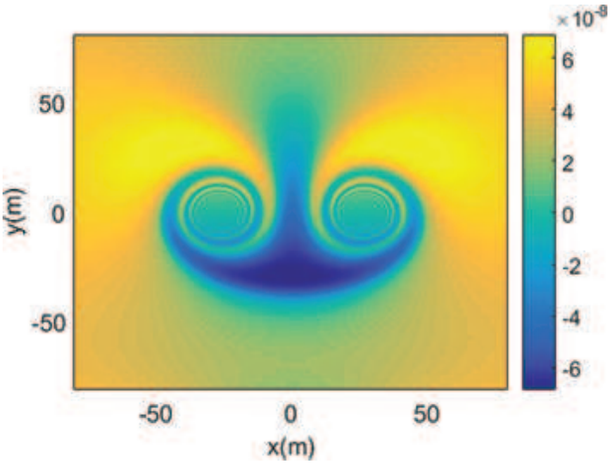

Figure 4. Dielectric constant distribution due to water vapour variation.

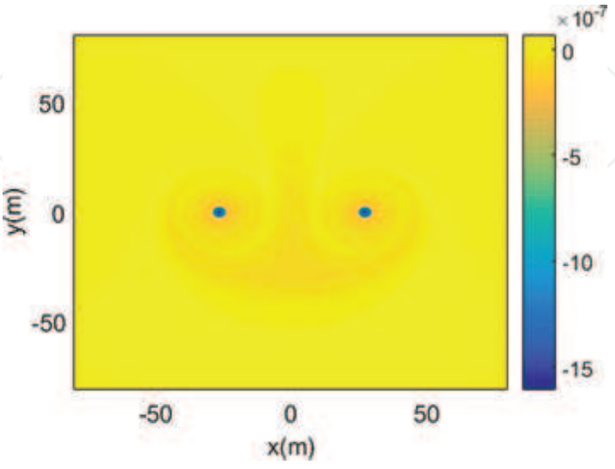

Figure 5. Total dielectric constant distribution.

http://dx.doi.org/10.5772/66544

2.5.1. Extrapolation of dielectric constant related to density distribution

As shown in Eq. (27), the key of density distribution is the integral $I(\mathbf{r})$; this could be obtained with the normalized parameters.

First, if the space is normalized by vortex separation b_0, say $\tilde{r} = r/b_0$, the Rankine model can be normalized as

$$V_\theta(r) = \frac{\Gamma_0}{b_0}\tilde{V}_\theta(\tilde{r}), \tag{37}$$

with $\tilde{V}_\theta$ being the normalized velocity:

$$\tilde{V}_\theta(\tilde{r}) = \frac{1}{2\pi\tilde{r}}\begin{cases}\tilde{r}^2/0.052^2, & \tilde{r}< 0.052,\\ 1, & \tilde{r}\geq 0.052.\end{cases} \tag{38}$$

Other velocity profile models have similar expressions. Substituting the normalized velocity into the integral Eq. (20) gives

$$I(\boldsymbol{r}) = \left(\frac{\Gamma_0}{b_0}\right)^2 \tilde{I}(\tilde{\boldsymbol{r}}) \tag{39}$$

Where the normalized integral $\tilde{I}(\tilde{\boldsymbol{r}}) = \int_{\tilde{C}} (\tilde{\boldsymbol{V}}\cdot\tilde{\nabla})\tilde{\boldsymbol{V}}\cdot \mathrm{d}\tilde{s}$ is only related to the velocity model, and $\tilde{\nabla} = (\partial/\partial\tilde{x} \quad \partial/\partial\tilde{y})^T = b_0\nabla$, $\overline{\mathbf{s}} = (\overline{x}, \overline{y})$.

For a stably flying airplane, the lift force balances the weight, which leads to the following initial circulation expression:

$$\Gamma_0 = \frac{Mg}{\rho_a V_a b_0} \tag{40}$$

Consequently, substituting the circulation into the integral gives

$$I(b_0\tilde{\boldsymbol{r}}) = \frac{M^2g^2}{\rho_a^2 V_a^2 b_0^4}\tilde{I}(\tilde{\boldsymbol{r}}) \tag{41}$$

The dielectric constant related to density distribution is then rewritten as

$$\Delta\varepsilon_r^d(b_0\tilde{\boldsymbol{r}}) \approx 1.552\times 10^{-6}\frac{R[T_a(b_0\tilde{\boldsymbol{r}}) + 4668q_a(b_0\tilde{\boldsymbol{r}})]}{\gamma p_a(b_0\tilde{\boldsymbol{r}})T_a(b_0\tilde{\boldsymbol{r}})}\frac{M^2g^2}{V_a^2 b_0^4}\tilde{I}(\tilde{\boldsymbol{r}}) \tag{42}$$

Since the normalized integral $\tilde{I}(\tilde{\boldsymbol{r}}) = \int_{\tilde{C}} (\tilde{\mathbf{V}}\cdot\tilde{\nabla})\tilde{\mathbf{V}}\cdot \mathrm{d}\tilde{s}$ is only related the velocity model, the following relationship can be obtained when the different airplane parameters and air conditions are introduced:

$$\frac{\Delta\varepsilon_{\mathrm{r},2}^{\mathrm{d}}(\boldsymbol{r}_2)}{\Delta\varepsilon_{\mathrm{r},1}^{\mathrm{d}}(\boldsymbol{r}_1)}\approx\frac{p_{\mathrm{a},1}(\boldsymbol{r}_1)T_{\mathrm{a},1}(\boldsymbol{r}_1)[T_{\mathrm{a},2}(\boldsymbol{r}_2)+4668q_{\mathrm{a},2}(\boldsymbol{r}_2)]}{p_{\mathrm{a},2}(\boldsymbol{r}_2)T_{\mathrm{a},2}(\boldsymbol{r}_2)[T_{\mathrm{a},1}(\boldsymbol{r}_1)+4668q_{\mathrm{a},1}(\boldsymbol{r}_1)]}\cdot\frac{M_2{}^2V_{\mathrm{a},1}{}^2b_{0,1}{}^4}{M_1{}^2V_{\mathrm{a},2}{}^2b_{0,2}{}^4} \tag{43}$$

with $\boldsymbol{r}_1 = b_{0,1}\tilde{\boldsymbol{r}}$ and $\boldsymbol{r}_2 = b_{0,2}\tilde{\boldsymbol{r}}$.

2.5.2. Extrapolation of dielectric constant related to water vapour distribution

The key of water vapour distribution is to solve the partial differentiation equation (33).

Define some related normalized parameters as follows: $\tilde{Q} = Q/b_0$,$\tilde{t} = t/t_0$,$\tilde{\boldsymbol{r}} = \boldsymbol{r}/b_0$,$\tilde{\mathbf{V}} = \mathbf{V}/V_0$, where $V_0 = \Gamma_0/b_0$ and $t_0 = b_0/V_0$. Consequently, the target partial differentiation equation is rewritten as

$$\frac{\partial\tilde{Q}}{\partial\tilde{t}} + (\tilde{\mathbf{V}}\cdot\ \tilde{\nabla})\tilde{Q} = -\tilde{V}_{\mathrm{y}}m_{\mathrm{q}}. \tag{44}$$

If the variable $\tilde{Q}(\tilde{\boldsymbol{r}},\tilde{t})$ is solved from above equation, the dielectric constant related to water vapour distribution becomes

$$\Delta\varepsilon_{\mathrm{r}}^{\mathrm{v}}(b_0\tilde{\boldsymbol{r}},t_0\tilde{t}) = 1.207\times10^{-2}\frac{p_{\mathrm{a}}}{T_{\mathrm{a}}^2}b_0\tilde{Q}(\tilde{\boldsymbol{r}},\tilde{t}). \tag{45}$$

In this manner, the dielectric constant for different airplane and air parameters is extrapolated as

$$\frac{\Delta\varepsilon_{\mathrm{r},2}^{\mathrm{v}}(\boldsymbol{r}_2,t_2)}{\Delta\varepsilon_{\mathrm{r},1}^{\mathrm{v}}(\boldsymbol{r}_1,t_1)}\approx\frac{p_{\mathrm{a},2}(\boldsymbol{r}_2)}{p_{\mathrm{a},1}(\boldsymbol{r}_1)}\left[\frac{T_{\mathrm{a},1}(\boldsymbol{r}_1)}{T_{\mathrm{a},2}(\boldsymbol{r}_2)}\right]^2\frac{b_{0,2}}{b_{0,1}} \tag{46}$$

where $\boldsymbol{r}_1 = b_{0,1}\tilde{\boldsymbol{r}}$, $\boldsymbol{r}_2 = b_{0,2}\tilde{\boldsymbol{r}} = \frac{b_{0,2}}{b_{0,1}}\boldsymbol{r}_1$, $t_1 = t_{0,1}\tilde{t}$, and $t_2 = t_{0,2}\tilde{t} = \frac{t_{0,2}}{t_{0,1}}t_1$. For stably flying airplane, we have $t_0 = \rho_{\mathrm{a}}b_0^3V_{\mathrm{a}}/(Mg)$, and then the relationship becomes

$$\frac{t_{0,2}}{t_{0,1}} = \left(\frac{b_{0,2}}{b_{0,1}}\right)^3\frac{p_{0,2}}{p_{0,1}}\frac{T_{0,1}}{T_{0,2}}\frac{V_{0,2}}{V_{0,1}}\frac{M_1}{M_2} \tag{47}$$

This is a very simple relationship.

With the combination of two extrapolation formulae, the dielectric constant distribution is then determined. This can save a lot of computation cost when different airplane wake vortices are to be analysed.

Another condition we always experience is wet weather condition (fog, rain, and snow). Here we mainly concern the rainy condition since it is the most common situation around airports.

http://dx.doi.org/10.5772/66544

3. Wake vortex generated in rainy weather

In still air, the raindrops fall vertically towards the ground and reach a constant terminal falling velocity. When an aircraft takes off or lands in rainy weather, the raindrops will be inevitably involved in the aircraft wake vortices. Raindrops' motion in wake vortex is modified by the vortex flow. This modification of the trajectories of the raindrops may induce changes in raindrops' number concentration and velocity distribution in wake vortices, therefore results in changes in the recorded radar signal. This section presents a modelling scheme for raindrops' motion and distribution within the wake vortex.

3.1. Parameterization of raindrops

In still air, a falling raindrop reaches its terminal fall velocity V_{T} with the equilibrium between the inertial force and the drag force acting on it [7]. A widely used exponential expression between V_{T}(m/s) and the diameter D(mm) is given by [8]

$$V_{\mathrm{T}}(D) = [\alpha_1 - \alpha_2 \exp(-\alpha_3 D)](\frac{\rho_0}{\rho})^{0.4} \tag{48}$$

where α_1 = 9.65 m/s, α_2 = 10.3 m/s, α_3= 0.6 m/s, and $(\rho_0/\rho)^{0.4}$ is a density ratio correction factor adjusting deviation of the terminal fall velocity due to the air density change with the fall altitude.

Drop size distributions (DSD) have been widely used by radar meteorologists as they are directly related to radar reflectivity [9]. In the following analysis, a suitable model to describe the size distribution of the rainfall in Europe is adopted [10]

$$N(D) = N_0 D^2 e^{-\Lambda D} \tag{49}$$

where N_0=64500$R^{-0.5}$ ($\mathrm{m^{-3}}$ $\mathrm{mm^{-3}}$) with R (mm/h) being the considered rain rate, $\Lambda = 7.09R^{-0.27}(\mathrm{mm^{-1}})$, $N(D)(\mathrm{m^{-3}mm^{-1}})$ represents the number of raindrops of the diameter D per unit volume per unit diameter class interval.

3.2. The motion equation of raindrops in wake vortices

Typically, the diameter of raindrops disperses between 0.5 and 4 mm. Usually their Stokes number in wake vortex flow is approximate to 1, which makes their motion trajectories significantly differ from the streamlines of total velocity field. To obtain those trajectories, the motion equation of the raindrops is studied [11].

When a raindrop enters into the wake vortex flow, its movement is governed by

$$a(t) = \frac{\mathrm{F_d}(t)}{m_{\mathrm{p}}} + g \tag{50}$$

where t is the time, a is the acceleration of the raindrop, F_d is the fluid drag force acting on the raindrop, m_{p} is its mass, and g is the gravity acceleration. For a raindrop moving with velocity

v_p in the fluid whose velocity field is $u[z_p(t)]$, if its diameter D ranges from 0.5 to 4 mm, the drag force F_d can be approximately considered in the Newton regime [12] and given by

$$F_d(t) = \frac{1}{2} C_d \rho_a \delta v^2 \left(\frac{\pi D}{2}\right)^2, \delta v = u[z_p(t)] - v_p(t) \tag{51}$$

where $z_p(t)$ denotes raindrops' position, δv is the relative velocity between the vortex flow and the raindrop, and C_d is the fluid drag coefficient. The impact of air density variations in the vortex flow on C_d can be neglected because the density of raindrops is much larger than that of air. Thus, C_d for a raindrop of diameter D is derived by the equilibrium equation of its weight and the drag force when falling at terminal falling velocity in still air:

$$C_d = \frac{4\rho_w g D}{3\rho_a V_T^2} \tag{52}$$

where ρ_w is the density of raindrops. Substituting Eqs. (51) and (52) into Eq. (50), the motion equation of raindrops within wake vortices can be further expressed as

$$\begin{cases} \boldsymbol{a}(t) = \boldsymbol{g} + \dfrac{\boldsymbol{g}}{V_T^2} |\delta \mathbf{v}| \delta \mathbf{v} \\ \dfrac{d\mathbf{v}_p(t)}{dt} = \boldsymbol{a}(t) \\ \dfrac{d\mathbf{z}_p(t)}{dt} = \mathbf{v}_p(t) \end{cases} \tag{53}$$

The instantaneous position and velocity of raindrops can be obtained from the above equations, but it is not easy to obtain a simple and closed expression. Here, a fourth-order four variables Runge-Kutta algorithm is proposed to solve the equation of motion [11].

3.3. Examples of trajectories of raindrops in wake vortices

In still air, the raindrop falls along a vertical trajectory to the ground. In presence of wake vortices, the trajectory of a raindrop is depending on its diameter and the location where it enters into the wake vortex flow. Circulation is a very important parameter to characterize wake vortex since it describes the strength of wake vortex. For raindrops moving in the vortex flow, their motion characteristics, that is, trajectory and velocity also largely depend on the vortex circulation. For simplicity, only the impacted part of the wake vortex region is shown in **Figure 6**, where four sets of trajectories are illustrated for raindrops of diameters 0.5, 1.0, 2.0, and 4.0 mm. Each set of trajectories corresponds to a given circulation value of the wake vortices. For a given circulation, the corresponding trajectory and velocity of raindrops in the wake vortices are unique. Comparisons between different trajectories give the following conclusions: (1) the smallest raindrops are much more sensitive to the vortex circulation and (2) the motion characteristic of raindrops in wake vortices is representative of the vortex strength.

http://dx.doi.org/10.5772/66544

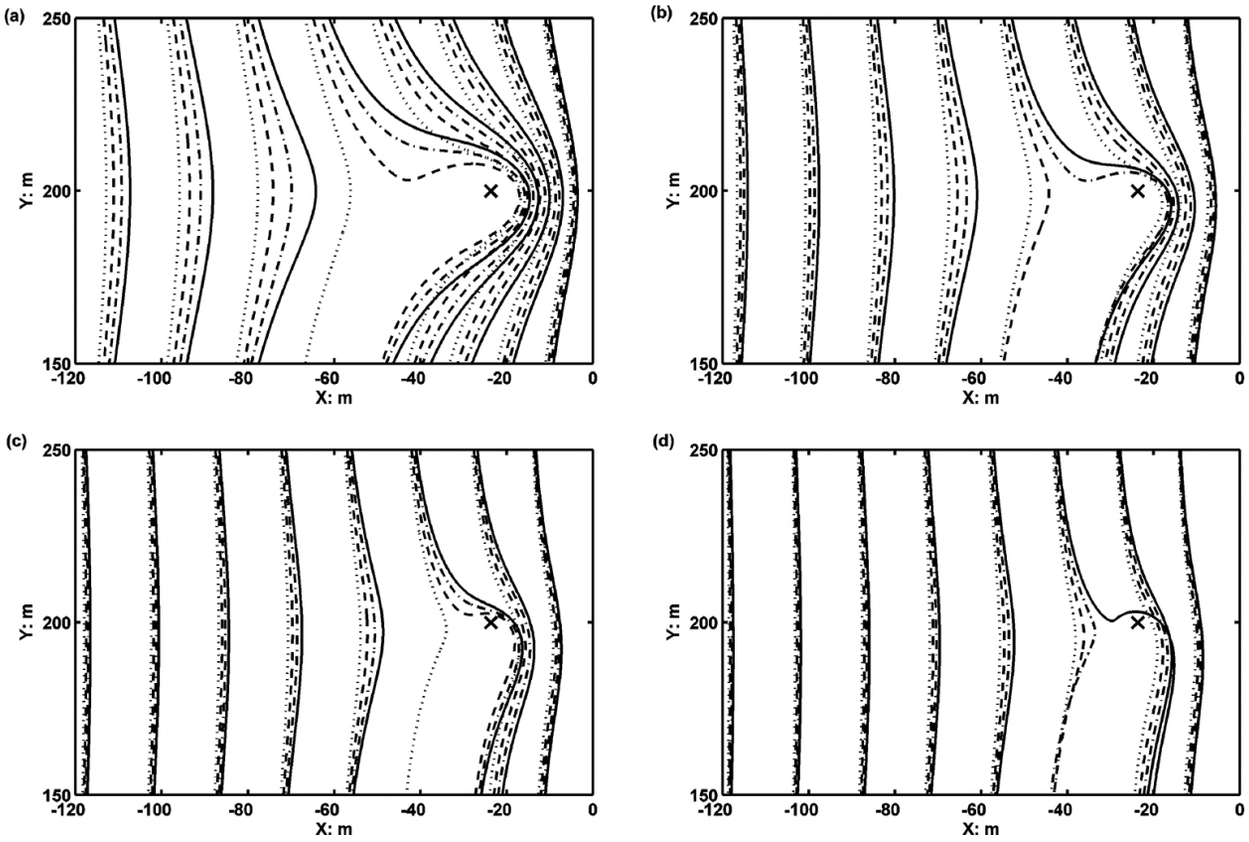

Figure 6. Raindrops' trajectories in wake vortices with different circulation: (a) D = 0.5 mm, (b) D = 1.0 mm, (c) D = 2.0 mm, (d) D = 4.0 mm. The solid line '-', the dash-dotted line '-.', the dashed line '–' and the dotted line '...', correspond to the values of vortex circulation: 490 m^2/s, 430 m^2/s, 360 m^2/s, and 300 m^2/s, respectively.

3.4. Raindrops' distribution in wake vortices

A Doppler radar will be very sensitive to raindrops' motion and possibly enable the detection of wake vortices in rain. To better understand the impact of wake vortices on the raindrops' motion, it is necessary to develop the methodology to quantitatively analyse the raindrops' distribution in wake vortices.

3.4.1. Raindrops' number concentration

The box counting method is adopted here to quantitatively compute raindrops' distribution in wake vortices. For simplification, we consider the situation where the raindrops are falling into the two dimensional rectangular region of wake vortex in stable phase. Before entering into the wake vortex region, the raindrops are falling in still air with the constant terminal falling velocity, and they are named as "initial raindrops". The number density of initial raindrops of diameter D (mm) is assumed to be $N_0(D)$ (m^{-3} mm^{-1}). In the wake vortex region, the raindrops' trajectory and velocity are changed and they are denoted as "disturbed raindrops". The number density of disturbed raindrops is assumed to be $N(D,x,y)$ (m^{-3} mm^{-1}), where (x, y) are the coordinates in the wake vortex region. Obviously, for a given wake vortex pair, $N(D,x,y)$depends on both the diameters of raindrops and their locations in wake vortex. In

order to better illustrate the influence of wake vortices on the raindrops' distribution, the raindrops' relative number concentration at a point (x, y) is defined as

$$\eta_N(D,x,y) = \frac{N(D,x,y)}{N_0(D)} \tag{54}$$

where $\eta_N(D,x,y)$ depicts the change in raindrops' concentration induced by the wake vortex. If $\eta_N > 1$, the concentration of raindrops is enhanced, otherwise it is reduced.

In order to obtain the quantitative estimation of η_N, the wake vortex region is divided into $n_x \times n_y$ grid boxes with equal size. The size of each grid box in xy plane are Δx and Δy, respectively. Above the wake vortex region, there are $n_x \times 1$ grid boxes where the initial raindrops of diameter D are homogeneously distributed, and the number of initial raindrops in each grid box is recorded as $\mathrm{Num}_0(D)$. At each time step, their positions and velocities are updated by computing the equation of motion. If some of the initial raindrops enter into the wake vortex region, the same number of new initial raindrops is added to the first row of the $n_x \times n_y$ grid boxes, say, the $n_x \times 1$ grid boxes above the wake vortex region. When all the raindrops released at initial time arrive at the bottom of wake vortex region, the number of disturbed raindrops $\mathrm{Num}(D,x,y)$ in each grid box in wake vortex region is counted. Thus, $\eta_N(D,x,y)$ can be approximated by the

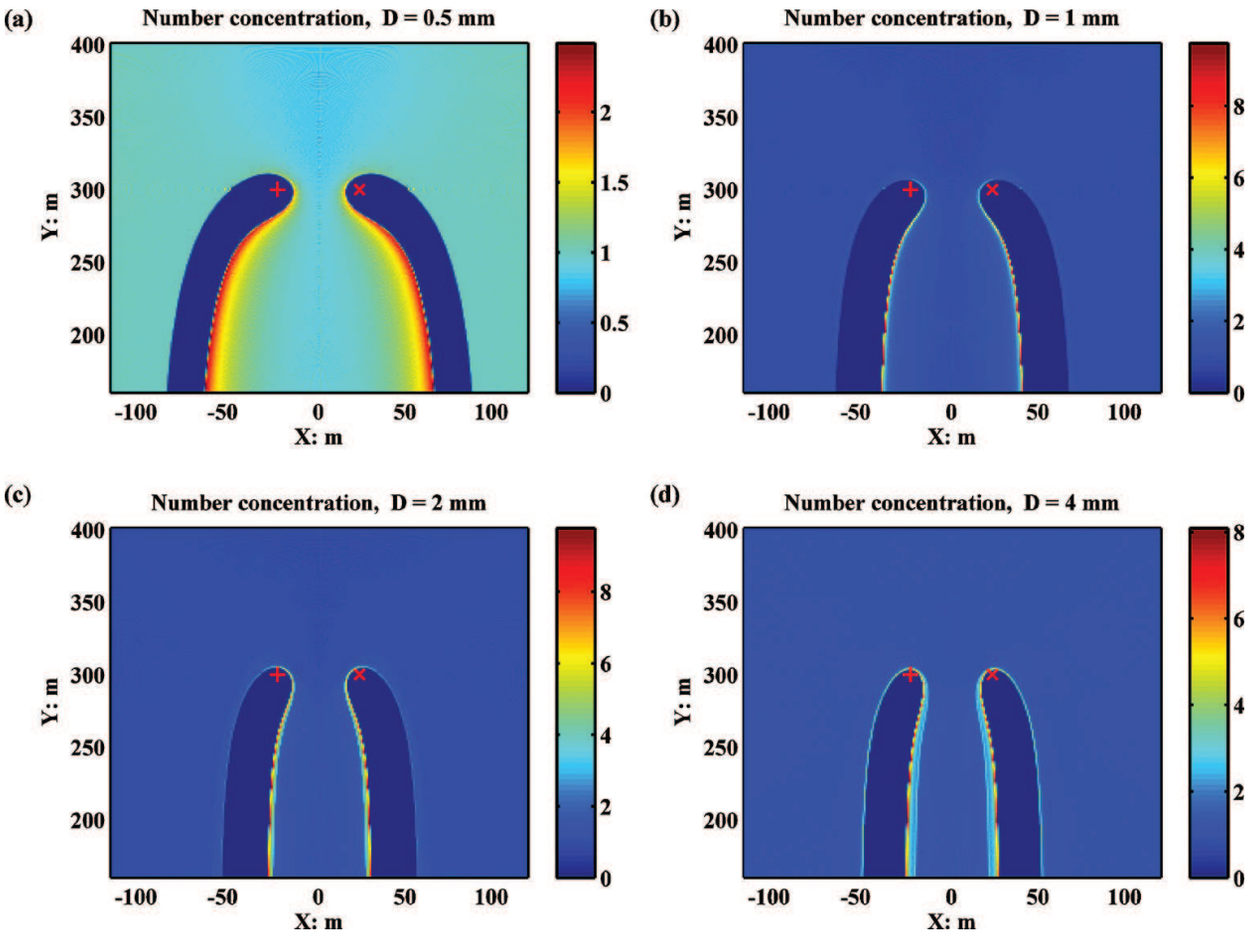

Figure 7. Raindrops' number concentration in wake vortices: (a) D = 0.5 mm, (b) D = 1.0 mm, (c) D = 2.0 mm, (d) D = 4.0 mm. The colour bar indicates the value of raindrops' number concentration in each grid box.

http://dx.doi.org/10.5772/66544

ratio of the number of disturbed raindrops in a grid box centred at (x, y) to the number of initial raindrops in a grid box above the wake vortex region, that is

$$\eta_N(D,x,y) = \frac{N(D,x,y)}{N_0(D)} \approx \frac{\mathrm{Num}(D,x,y)}{\mathrm{Num}_0(D)} \tag{55}$$

Obviously, the estimation accuracy of $\eta_N(D,x,y)$ depends on the choice of the grid box size: Δx and Δy, and the number of initial raindrops in each grid box above the wake vortex region: $\mathrm{Num}_0(D)$.

Parameters	Values
Aircraft wingspan	60.30 m
Aircraft maximum landing weight	259,000 kg
Aircraft landing speed	290 km/h
Grid box size	1 m × 1 m
$\mathrm{Num}_0(D)$	100
Raindrops' diameter	0.5 mm, 1.0 mm, 2.0 mm, and 4.0 mm

Table 2. Parameters for the computation of raindrops' number concentration.

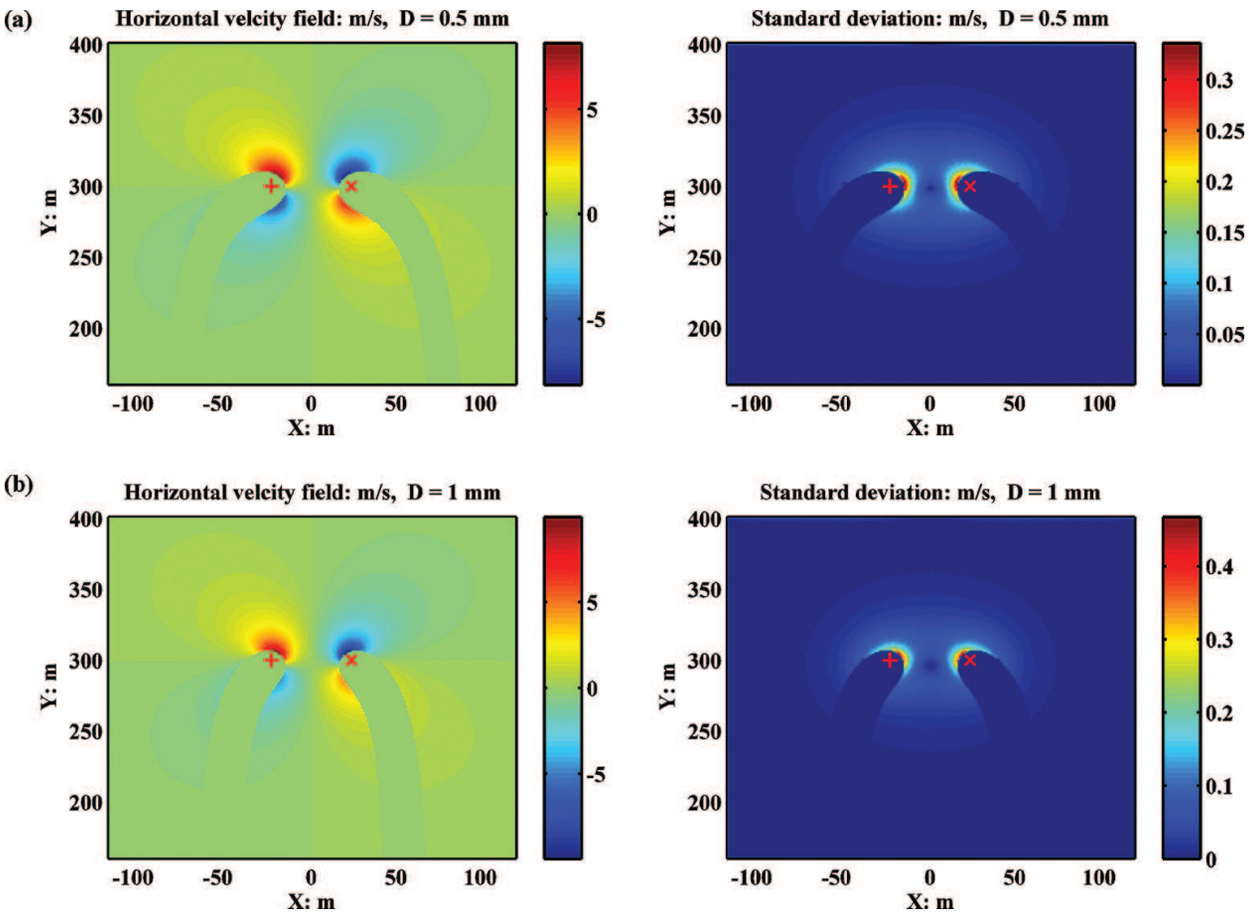

Figure 8. Raindrops' horizontal velocity distribution in wake vortices: (a) D = 0.5 mm and (b) D = 1.0 mm.

In **Figure 7**, the raindrops' number concentration in wake vortices is illustrated. The simulation parameters are listed in **Table 2**. It can be noticed that in the wake vortex region, there are two columns where the raindrops' concentration is very small, even to zero. These two columns appear symmetrically below the two vortex cores and the distance between them in (a) is much wider than the others. Between these two columns, there are two narrow regions where the number concentration of raindrops is enhanced. For the raindrops of 1 and 2 mm of diameter, the number concentration value exceeds 8 in some grid boxes.

3.4.2. Raindrops' velocity distribution

Besides the number concentration, the raindrops' velocity distribution in each grid box is of great interest. If the grid box size used for the box counting method is small enough and the number of raindrops in each grid box is large enough, the velocity components of the raindrops in one grid box can be thought to obey Gaussian distributions. The mean value and variance of the velocity of the raindrops in each grid box are computed. If the number concentration of the grid box is zero, the raindrops' velocity in this grid box is set to 0.

In **Figures 8** and **9**, the raindrops' horizontal and vertical velocity distribution in wake vortices are illustrated, respectively. From **Figure 8**, it is interesting to find that the raindrops'

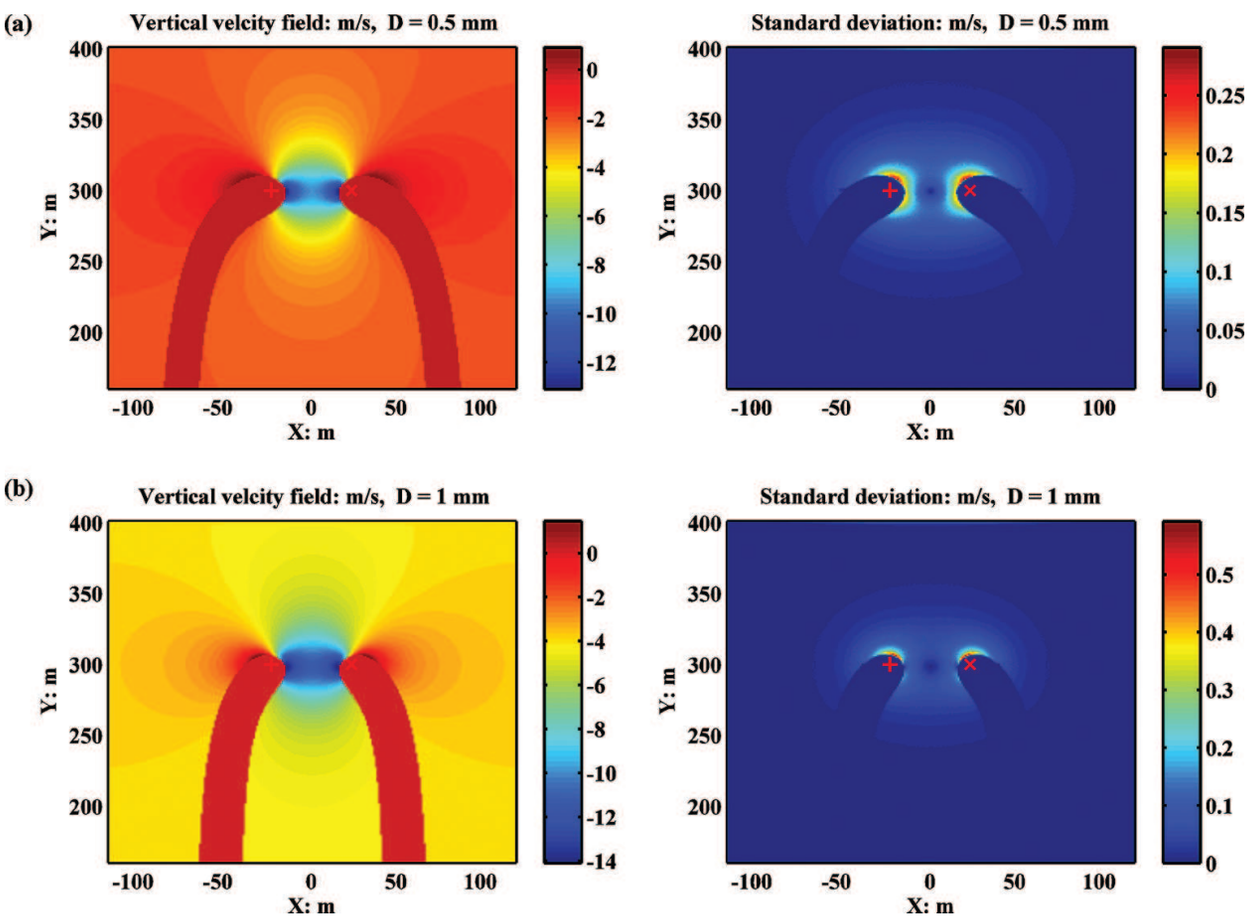

Figure 9. Raindrops' vertical velocity distribution in wake vortices: (a) $D = 0.5$ mm and (b) $D = 1.0$ mm.

http://dx.doi.org/10.5772/66544

horizontal velocity field is similar to the wake vortex velocity field. From **Figure 9**, it is interesting to find that between the two vortex cores, the raindrops' vertical velocity is speeded up. At the same time, the standard deviation of the raindrops' velocity distribution in a grid box is sufficiently low to consider it as constant within each grid box. In fact, in wake vortex, the raindrops' motion is affected by the vortex flow; the raindrops' velocity field is not the same as the superimposition of the vortex flow velocity and raindrops' terminal velocity, but it is representative of the wake vortex velocity characteristics.

Author details

Jianbing Li[1]*, Zhongxun Liu[2] and Xuesong Wang[3]

*Address all correspondence to: jianbingli@nudt.edu.cn

1 College of Electronic Science and Engineering, National University of Defence Technology, Changsha, China

2 National Key Laboratory of Airspace Technology, Beijing, China

3 College of Science, National University of Defense Technology, Changsha, China

References

[1] Thayer, G.D. An improved equation for the radio refractive index of air. Radio Science. 1974; **9**(10):803–807.

[2] Anderson, J. D. Introduction to Flight. McGraw-Hill College; New York, 2004.

[3] Gerz T., Holzapfel F., and Darracq D. Commercial aircraft wake vortices. Progress in Aerospace Sciences. 2002; **38**(3):181–208.

[4] Myers, T. J. and Scales, W. A. Determination of aircraft wake vortex radar cross section due to coherent Bragg scatter from mixed atmospheric water vapor. Radio Science. 1999; **34**(1):103–111.

[5] Streeter, V. L., Wylie, E. B., and Bedford, K. W. Fluid Mechanics. McGraw-Hill; New York, 1997.

[6] Anderson, J. D. Computational Fluid Dynamics: The Basics with Applications. McGraw-Hill; New York, 1995.

[7] Sauvageot, H. Radar Meteorology. Artech House Publishers; London, 1992.

[8] Bringi, V. N. and Chandrasekar, V. Polarimetric Doppler Weather Radar: Principles and Applications. Cambridge University Press; Cambridge, 2004.

[9] Marshall, J. S. and Palmer, W. M. The distribution of raindrops with size. Journal of Meteorology, **5**: 165–166, 1948.

[10] Owolawi, P. A. Characteristics of Rain at Microwave and Millimetric Bands for Terrestrial and Satellite Links Attenuation in South Africa and Surrounding Islands. PhD thesis, University of KwaZulu-Natal, KwaZulu-Natal, South Africa, 2010.

[11] Zhongxun, L. I. U. Modélisation des signatures radar des tourbillons de sillage par temps de pluie. PhD thesis, University of Toulouse, Toulouse, 2013.

[12] Lovejoy, S. and Schertzer, D. Turbulence, raindrops and the l1/2 number density law. New Journal of Physics, **10**: 075017 (32pp), 2008.